

Hydrogen-Bond Transition from the Vibration Mode of Ordinary Water to the (H, Na)I Hydration States: **Molecular Interactions and Solution Viscosity**

Yong Zhou¹, Yongli Huang^{2,*}, Lei Li¹, Yinyan Gong³, Xinjuan Liu³, Xi Zhang⁴, Chang Q Sun^{1,5,*}

Abstract

With the aid of differential phonon spectrometrics (DPS) and surface stress detection, we show that HI and NaI solvation transforms different fractions of the H-O stretching phonons from the mode of ordinary water centred at ~ 3200 to the mode of hydration shell at ~ 3500 cm^{-1} . Observations suggest that an addition of the $\text{H} \leftrightarrow \text{H}$ anti-hydrogen-bond to the Zundel notion, $[\text{H}(\text{H}_2\text{O})_2]^+$, would be necessary as the H-O bond due H_3O^+ has a 4.0 eV energy, and the $\text{H} \leftrightarrow \text{H}$ fragilization disrupts the solution network and the surface stress. The I^- and Na^+ ions form each a charge centre that aligns, stretches, and polarize the O:H-O bond, resulting in shortening the H-O bond and its phonon blue shift in the hydration shell or at the solute-solvent interface. The solute capabilities of bond-number-fraction transition follow: $f_{\text{H}} = 0$, $f_{\text{Na}} \propto C$, and $f_{\text{I}} \propto 1 - \exp(-C/C_0)$ toward saturation, with C being the solute molar concentration and C_0 the decay constant. The $f_{\text{H}} = 0$ evidences the non-polarizability of the H^+ because of the $\text{H} \leftrightarrow \text{H}$ formation. The linear $f_{\text{Na}}(C)$ suggests the invariance of the Na^+ hydration shell size because of the fully-screened cationic potential by the H_2O dipoles in the hydration shell but the nonlinear $f_{\text{I}}(C)$ fingerprints the $\text{I}^- \leftrightarrow \text{I}^-$ interactions at higher concentrations. Concentration trend consistency between Jones–Dole’s viscosity and the $f_{\text{Na}}(C)$ coefficient may evidence the same polarization origin of the solution viscosity and surface stress.

¹ Key Laboratory of Extraordinary Bond Engineering and Advanced Materials Technology (EBEAM), Yangtze Normal University, Chongqing 408100, China (20161042@yznu.cn; leili13@126.com)

² School of Materials Science and Engineering, Xiangtan University, Xiangtan 411105 (huangyongli@xtu.edu.cn)

³Institute for Coordination Bond Engineering, China Jiliang University, Hangzhou 310018, China (14A0502088@cjlu.edu.cn; yqong2007@gmail.com)

⁴ Institute of Nanosurface Science and Engineering, Shenzhen University, Shenzhen 518060, China; (Zh0005xi@szu.edu.cn)

⁵ NOVITAS, Nanyang Technological University, Singapore 639798 (ecqsun@ntu.edu.sg)

1. Introduction

Solvation of acid and salt, taking HI and NaI as representatives, is of ubiquitously important to fields such as biochemistry, organic chemistry, food and medicine, health care and life quality of human beings [1-3]. However, it remains yet uncertain how the H^+ , Na^+ and I^- solvation transform their respective hydrogen-bond network, or the solute-solvent interface bonding dynamics, despite intensive investigations made since centuries long ago [4] with focus mainly on the solute diffusive motion dynamics [5], hydration-shell thickness [6, 7], characteristic phonon life time [8-11], and interface dipole orientation [12, 13].

The proton mobility in acid solutions was explained firstly by Grotthuss [4] two-century ago in terms of 'structural diffusion' that was subsequently refined by invoking mechanisms of thermal hopping [14], proton tunnelling [15], and fluctuating [16]. In 1960s, Eigen [17] proposed an H_9O_4^+ complex in which a H_3O^+ core is strongly hydrogen-bonded to three H_2O molecules and leaves its lone pair free. Zundel [18] proposed a $[\text{H}(\text{H}_2\text{O})_2]^+$ in which the proton is shuttling alternatively between two H_2O molecules. From the *ab initio* path integral simulations, Marx et al [19] noted that the hydrated proton forms a fluxional defect in the hydrogen-bonded network, with both $[\text{H}(\text{H}_2\text{O})_2]^+$ and $[\text{H}(\text{H}_2\text{O})_4]^+$ occurring only in the sense of 'limiting' or 'ideal' structures. The defect can become delocalized over several hydrogen bonds owing to quantum fluctuations.

An ultrafast 2DIR spectroscopy investigation [10, 20] suggested that the proton prefers the manner of Zundel structure accommodated by two H_2O at a time, rather than the Eigen structure in which the protons piggyback on individual molecules. In contrast, another work [11] favours deuterated prototypical Eigen clusters, $[\text{H}(\text{D}_2\text{O})_4]^+$, bound to an increasingly basic series of hydrogen bond acceptors. By tracking the frequency of every O-D stretch vibration in the complex as the transferring hydrogen is incrementally pulled from the central hydronium to a neighbouring water molecule. Clearly, debate on proton performance continues. However, we should focus not only on the proton performance but also its capabilities of transforming the solution matrix bonds and electrons and the solute-solvent interface bonding dynamics and the solution-surface performance.

Salt solvation not only changes the surface stress of the solution but also varies the solution ability of dissolving proteins, which has been explained from perspectives of interaction length scales [21], ionic specificity [22, 23], ion-skin induction [24], quantum dispersion [25], structural order and disorder making [21, 26-29], etc. Based on measurements of 1 M potassium halide solutions with 14 mol % HOD in D₂O, Smith et al [30] contended that the Raman ω_H blue shift for the salt solutions from that of the deionized water arises primarily from the electric fields rather than from rearrangement of the hydrogen bonds beyond the first hydration shell or from structure breaking [31].

Recent MD computations [32] suggested that an external fields in the 10^9 V/m order can slow down water molecules and even crystallize the system. The fields generated by the Na⁺ ions act rather locally but can reorient the hydrated neighbouring water molecules. MD computations [33] also suggested that HCl hydration make water clusters into smaller ones by fragmentation.

Recent progress [34-37] demonstrated that serving as charge centres, the (Li, Na, K, Rb, Cs)⁺ cations and the (Cl, Br, I)⁻ anions in alkali halide solutions form each a polarization centre that aligns and clusters water molecules, and stretches the neighbouring hydrogen bonds. The only difference between the cations and anions upon solvation is that the cation hydration shell is smaller than those of the anions and the opposite directions of the electric fields. Ionic polarization shortens and stiffens the H-O bonds and meanwhile lengthens and softens the O:H nonbonds in the hydration shells, resulting in the respective H-O phonon frequency blue shift and O:H phonon frequency redshift [34, 36]. However, little is known yet on the ionic and protonic effect on transforming the solution matrix hydrogen bond upon acid and salt solvation though the solute behaviour has been well understood [3, 10, 11, 19].

With the aid of the Raman differential phonon spectrometrics (DPS) and the contact angle measurements, we show herewith comparatively how the H⁺, Na⁺ and I⁻ react with the solution hydrogen bonds and how the DPS can resolve solute capabilities of transforming the solution bonds from the mode of ordinary water to the hydration shells and how the transformed bond relaxes.

2. Principles and processes

2.1. Phonon frequency and spectroscopy

A phonon spectral peak features the Fourier transformation of all bonds vibrating in the same frequency irrespective of their locations or orientations in the solid, liquid, or vapour phase of a substance. One can only probe the statistic mean of the vibrations and its fluctuation. The phonon frequency features the respective bond stiffness, $\omega_x^2 \propto E_x/d_x^2$, (bond stiffness is the product of its elasticity Y and length d , $Yd = Ed/d^3$, energy density times bond length) [38]. The ω_x , E_x and d_x are the phonon wavenumber shift, O:H-O segmental energy and length, respectively. The subscript $x = L$ and H denotes the respective O:H and the H-O segment. The spectroscopy probes intrinsically the change of the bonding identities without being able to discriminate the sources of stimuli. Dominating the spectral peaks shift, the O:H-O bond segmental length and energy vary in the same H-O elongation and O:H contraction manner under mechanical compression and base solvation [39], and the other way around under liquid heating [40], compressing [41], salting [42], and molecular undercoordination, [38] as well.

As compared in Figure 1, we collected the full-frequency Raman spectra for NaI/H₂O and HI/H₂O solutions at different molar concentrations (or molecular number ratios that could be more convenient than using mole per litre water) with respect to the spectrum of deionized water probed under the same conditions. Evolution of the characteristic peaks for the O:H and the H-O stretching vibration centered at $< 200 \text{ cm}^{-1}$ and at $>3000 \text{ cm}^{-1}$, respectively, would suffice to examine the O:H-O segmental cooperativity, so one can omit the rest modes due to bond bending and torsional motion for simplicity. The bending and torsional vibrations are featured in the $300\text{-}1600 \text{ cm}^{-1}$, which contributes insignificantly to the O:H-O cooperative stretching vibrations that follow the $\omega_x^2 \propto E_x/d_x^2$ relation. From the full-frequency Raman spectra, one could hardly be able to gain quantitative information on the solvation transformed stiffness, fraction, and fluctuation of bonds from the mode of ordinary water to the hydration shell in the solution network.

2.2. Solvation dynamics and full-frequency Raman spectroscopy

NaI and HI solvation proceeds in the following ways:

$\text{NaI} + \text{H}_2\text{O} \Rightarrow \text{Na}^+ + \text{I}^- + \text{H}_2\text{O}$ (polarization with O:H elongation and H-O contraction [42])

$\text{HI} + 2\text{H}_2\text{O} \Rightarrow \text{I}^- + (\text{H}^+ + 2\text{H}_2\text{O}) \Rightarrow \text{I}^- + [\text{H}(\text{H}_2\text{O})_2]^+$ (H_3O^+ and $\text{H} \leftrightarrow \text{H}$ anti-HB formation [36])

Figure 1a inset illustrates the ionic polarization of water molecules [38]. Serving as the point charge centre, ions form each an electric field pointing outwardly for cation or inwardly for anion. The field aligns, clusters, stretches and polarizes surrounding water molecules to form the hydration shells. The polarized dipoles lined oppositely along the field, and at higher concentration, solute-solute interaction comes into play, which weakens the field in the hydration shells. The resultant field shortens the H-O bond and stiffens its phonon from the bulk mode centered at 3200 to the hydration-shell mode at 3500 cm^{-1} , lengthens the O:H nonbond and softens its phonon from the bulk mode at ~ 200 to the shell at ~ 75 cm^{-1} . The polarization raises the solution elasticity and surface stress. The polarization ability of a cation is weaker than an anion and ions of larger radius and lower electronegativity effect more significant as Hofmeister noted [43].

Figure 1b inset illustrates the H_3O^+ formation that substitutes for the central H_2O molecule in the $2\text{H}_2\text{O}$ unit cell [36]. The H^+ dissolved from acid solvation binds to the H_2O firmly to form a H_3O^+ tetrahedron by sharing one of the two lone pairs of the oxygen. Unlike Na^+ that can be dissolved from NaCl at 150 K temperature or even below [44], the H-O bond of ≥ 4.0 eV cohesive energy [43] requires 121.6 nm UV laser excitation to break [45].

On the other hand, for a water specimen having N oxygen atoms, there will be $2N$ bonded protons and $2N$ lone pairs. Each of the lone pair “:” or the H^+ has 50% probability to interact with protons or lone pairs of the neighbour water molecules. This regulation allows only for the O:H-O formation between oxygen ions tetrahedrally coordinated in ordinary water. The introduction of a H_3O^+ hydronium into the specimen of N oxygen ions will break the $2N$ conservation and the O:H-O configuration by adding turning the $2N$ protons into $2N+1$ and the $2N$ lone pairs into $2N-1$. Thus, the excessive two protons form the $\text{O}-\text{H} \leftrightarrow \text{H}-\text{O}$, named anti-hydrogen-bond (anti-HB) [36]. The anti-HB disrupts the solution network and depresses the surface stress of acid solutions.

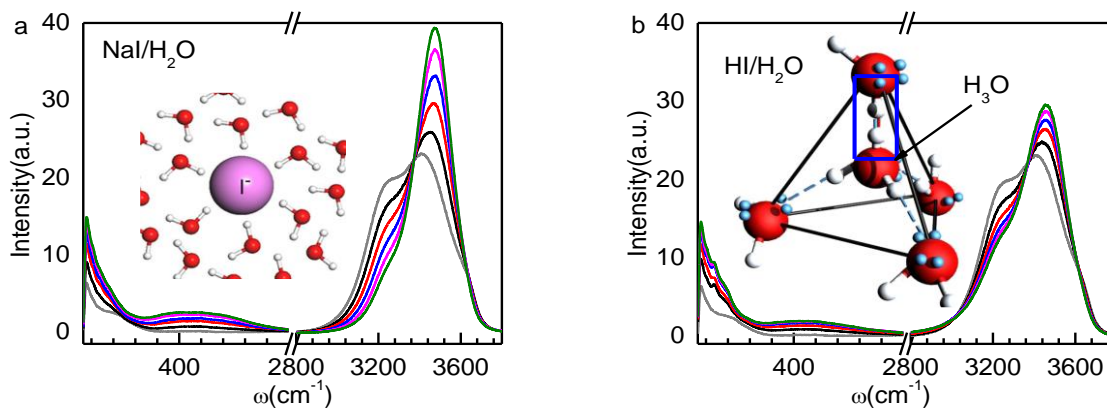


Figure 1. Concentration dependence of the full-frequency Raman spectroscopy for (a) NaI and (b) HI solutions with concentration varying from 0.02 to 0.10 molar fraction (number ratio will be more convenient than using the unit of M/L) . Inset **a** illustrates the process of ionic polarization that stiffens the H-O phonon and softens the O:H phonons because of the O:H-O bond cooperativity. Inset **b** shows the structure unit cell of water with a H_3O^+ replacement for the central H_2O upon HI solvation. The framed $\text{H}\leftrightarrow\text{H}$ anti-hydrogen-bond prevents H^+ from being able to polarize its neighbours or from translational tunnelling between water molecules, but serves as a point breaker disrupting the hydrogen network and the surface tension of the acidic solutions.

3. Results and discussion: DPS derivatives

3.1. DPS derivatives

In order to calibrate the solute capability of polarization, one can subtract the specific H-O and O:H segmental spectral peaks of the solutions by the referential characteristic peaks of deionized water upon both sets of spectral peak area being normalized. The normalization excludes the artifacts of measurements and to ensure that the phonon abundance remain constant – the loss equals to its gain upon hydration[38], and furthermore, avoid the peak decomposition with uncertain number of components. As an artifact of the measurements, the difference of the Raman mode cross-section between the conditioned and the ionized water can be removed by the spectral peak area normalization though the difference was estimated in the 10^{-3} order [46]. The DPS needs

no background correction as all the spectral minimum is at zero, otherwise, correction could be added with reference to that of pure water.

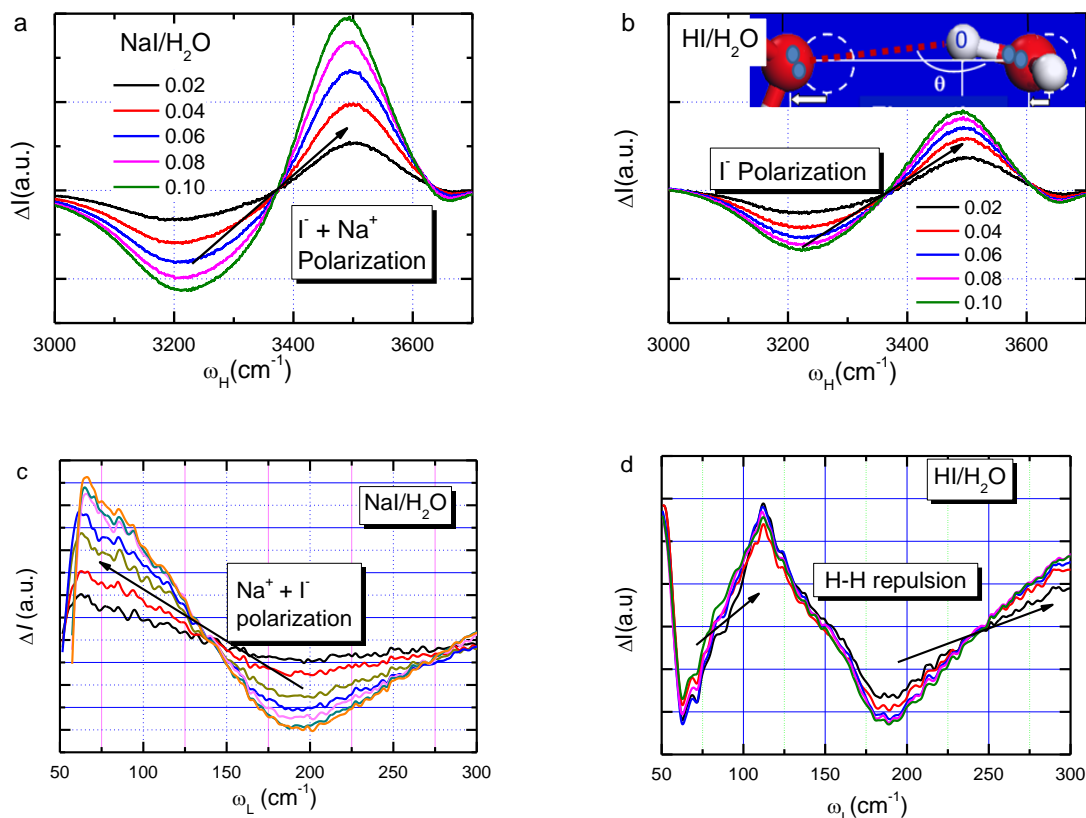


Figure 2. The concentration-resolved ω_x DPS for (a, c) NaI/H₂O and (b, d) HI/H₂O solutions. The Na⁺ and I⁻ polarization lengthens the O:H nonbond and softens its phonons and meanwhile shortens the H-O bond and stiffens its phonon from the mode of the ordinary water ~ 3200 to the mode of the hydration shell at ~ 3500 cm^{-1} with different abundances as inset b compares. The ω_L shift resolves the effects of ionic polarization that weakens the O:H from the H \leftrightarrow H repulsion that reverse the polarized O:H nonbond.

Figure 2 compares the ω_x DPS for the H-O bonds conditioned by HI and NaI solvation. The peak above the x-axis is the abundance gain that equals its loss below the x-axis due to solvation.

Results in Figure 2a and b compare the effects of NaI and HI solvation on H-O bond relaxation.

HI and NaI solutes have the same effect on stiffening the ω_H from 3220 to ~ 3500 at varied

abundance of transformation. HI solvation transmits less the H-O phonon abundance than the NaI does, discriminating the effect of Na^+ and H^+ on the amount of the network O:H-O bond polarization.

The ω_L DPS in Figure 2c, d show that the O:H stretching phonons undergo a cooperative redshift because of the O:H-O bond cooperativity. The ionic polarization shifts the O:H phonon from the water mode at ~ 180 to the hydration-shell mode at $\sim 75 \text{ cm}^{-1}$ but the $\text{H} \leftrightarrow \text{H}$ repulsion reverses the shift from 75 to 120 cm^{-1} and from 180 to above 250 cm^{-1} .

3.2. Bond transition, polarization and fragilization

The integral of the normalized peak sums all the detectable bonds in solution, which is taken as unity. The DPS distills the fraction (< 1 unity) of phonons or bonds transforming from the mode of ordinary water to the hydration shell upon solvation. The DPS removes the spectral area commonly shared by the mode of the ordinary water and the hydration shell but it is out of immediate concern. The commonly shared area may contain the high-order hydration shells of weak polarization, so the DPS peak arises mainly from the solute-solvent interface, which is the advantage of the DPS.

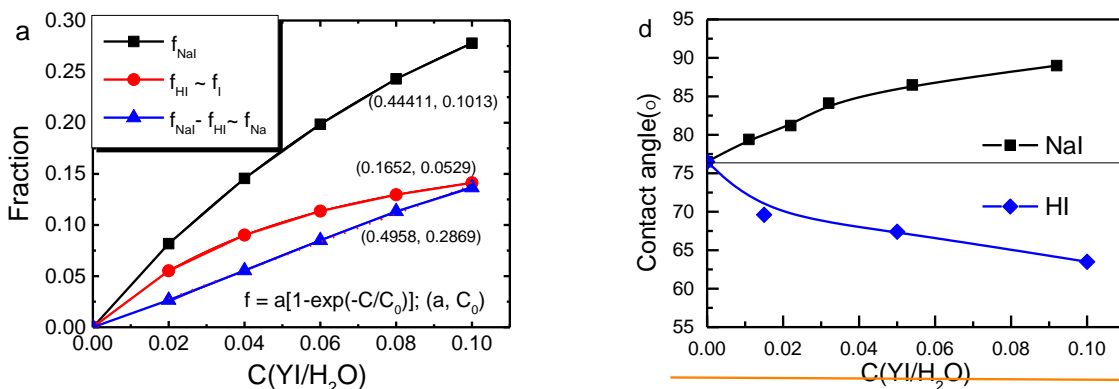


Figure 3. Concentration dependence of the (a) fraction coefficient as an integral of transformed hydration-shell phonons and (b) contact angles between the NaI and the HI solutions and glass substrate evidence the $\text{H} \leftrightarrow \text{H}$ disruption of the acid solution bonding network and surface stress and the ionic polarization raised surface stress. The coefficient features the fraction of the H-O

phonons or the H-O bonds being transformed from the ordinary water to the hydration shell by solvation. Fitting in the form of $f = a[1-\exp(-C/C_0)]$ separates the effect of f_{Na} from f_I with justification of $f_H = 0$.

Figure 3a compares the fraction coefficients for I^- , Na^+ , and NaI capabilities of transforming the fraction of H-O bonds being detected with provision of the justified $f_H = 0$ [36]. The $H \leftrightarrow H$ formation disables the H^+ for polarization, thus $f_{HI} = f_I$ and $f_{NaI} - f_I = f_{Na}$. The $f_{Na} < f_I$ and the f_{Na} varies nearly linearly with solute concentration till its concentration limit at ~ 0.1 ; the f_I , however, varies exponentially towards saturation, according to the best fit. It is noted that the slope of the $f(C)$ corresponds to the number of H_2O molecules per solute. The nearly linear dependence of the f_{Na} implies the invariance of the Na^+ hydration shell size or the solute electric field that is screened by the opposite aligned dipoles in the hydration shells.

Figure 3b shows the concentration dependence of the contact angle between the solutions and glass substrates, which features the solute capability of transforming the surface stress as an indication of polarization [34-36]. Here we focus on the concentration trends of the solute capability of transforming the surface stress of the solution rather than the solution-substrate interaction that is out of the present concerns. Observations confirm that the $H \leftrightarrow H$ anti-HB disruption takes the full responsibility for depressing the surface stress and the dilutive and corrosive properties of acid solutions but ionic polarization by salt solvation raises the solution viscoelasticity and surface stress, instead [35]. Results are consistent with MD calculations [32, 33] on the hydration shell molecular slow dynamics and the H^+ induced network fragilization.

3.3. Molecular interactions and viscosity

The invariance cationic shell size indicates that the cationic field is fully screened by water dipoles so the cationic solute is subject none to the interference of other solutes. However, the fast concentration decay of the f_I indicates that the $I^- - I^-$ repulsion comes into play, which weakens the local electric field in the hydration shells. The discrepancy in ionic surface area, $(R_I/R_{Na})^2 \sim (2.2/1.0)^2 \sim 5$, indicates that the number of H_2O dipoles attached to the I^- is insufficient to fully screen the I^- solute that is subjecting to interference of other I^- anions. The interference becomes stronger

when the solute concentration increases. Therefore, only anion-anion interactions and the solute-solvent interactions exist in alkali halide solutions.

One may note that the relative viscosity due to salt solvation is proportional to the fraction $f(C)$ of O:H-O bonds transiting from the mode of water to the hydration shells of the solutes. One can adjust the factor A and B in the Jones–Dole expression [47] to match the $f(C)$ curves in Figure 4 for NaI and NaCl:

$$\frac{\Delta\eta(C)}{\eta(0)} = A\sqrt{C} + BC \cong f(C) \quad (\text{Jones – Dole})$$

$$f(C) = a[1 - \exp(-C/C_0)] \quad (\text{Fraction – Coefficient})$$

It is thus clear that the viscosity is proportional to the extent of polarization or the fraction of O:H-O bonds transiting from the water mode to the hydration shells. Therefore, polarization dictates not only the surface stress but also the solution viscosity. Solute overdosing makes both the relative viscosity and the $f(C)$ towards saturation because of the anion-anion interaction.

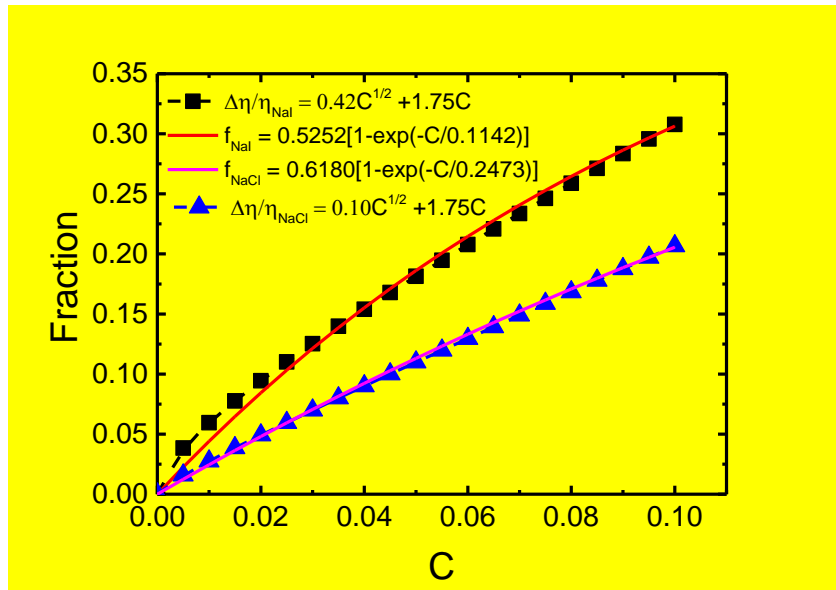


Figure 4. Correlation between the relative viscosity and the fraction coefficient for Na(I, Cl) solutions as a function of molar concentration. The NaCl data is derived from [48].

4. Conclusion

We show quantitatively that the H^+ hardly forms a hydration shell or polarizes H_2O molecules because of the H_3O^+ formation with 4.0 eV H-O bond energy. An addition of the $\text{H}\leftrightarrow\text{H}$ anti-HB to the Zundel $[\text{H}(\text{H}_2\text{O})_2]^+$ notion would be necessary as the $\text{H}\leftrightarrow\text{H}$ disrupts the solution network and the surface stress, discriminating the HI from the NaI solutions. In contrast, Na^+ and I^- ions form each a polarization centre that shortens and stiffens the H-O bond, and meanwhile, lengthens and softens the O:H nonbond via O-O coulomb repulsion. The resultant of I^- and Na^+ polarization and $\text{I}^- \leftrightarrow \text{I}^-$ repulsion stem the cooperative O:H and H-O phonon frequency. The fraction of phonons being transformed by H^+ , Na^+ and I^- ions follows the relationship: $f_{\text{H}} = 0$, $f_{\text{Na}} \propto C$, and $f_{\text{I}} \propto 1 - \exp(-C/C_0)$ towards saturation. The invariance of the $f_{\text{Na}} \propto C$ slope indicates that the tiny Na^+ is subject interference of other solutes because it is fully-screened by its surrounding hydrating H_2O dipoles. The consistency of the concentration trend of the solution viscosity and the f_{NaI} suggest that the ionic polarization stem the increase of both the solution viscosity and surface stress. Being able to resolve solute capabilities of hydrogen-bond and surface stress transformation, the DPS could be one of the powerful tools to probe comprehensive information on processes taking place in aqueous solutions without needing any assumption.

Acknowledgement

Financial support received from the National Natural Science Foundation (No.: 11502223) of China, the Natural Science Foundation of Hunan Province (No. 2016JJ3119), the Natural Science Foundation of Shen Zhen (No. 827000131), and **Science Challenge Project (No. TZ2016001)**.

Notes and references

1. N. Agmon, H.J. Bakker, R.K. Campen, R.H. Henchman, P. Pohl, S. Roke, M. Thämer, and A. Hassanali, *Protons and Hydroxide Ions in Aqueous Systems*. Chemical Reviews **116**(13): 7642-7672 (2016).
2. A.S. Amarasekara, *Acidic Ionic Liquids*. Chem Rev (2016).
3. E. Codorniu-Hernández and P.G. Kusalik, *Probing the mechanisms of proton transfer in liquid water*. Proceedings of the National Academy of Sciences **110**(34): 13697-13698 (2013).
4. C. de Grotthuss, *Sur la Décomposition de l'eau et des Corps Qu'elle Tient en Dissolution à l'aide de l'électricité*. Galvanique. Ann. Chim (1806).
5. D. Decka, G. Schwaab, and M. Havenith, *A THz/FTIR fingerprint of the solvated proton: evidence for Eigen structure and Zundel dynamics*. Physical Chemistry Chemical Physics **17**(17): 11898-11907 (2015).
6. R. Shevchuk, N. Agmon, and F. Rao, *Network analysis of proton transfer in liquid water*. The Journal of chemical physics **140**(24): 244502 (2014).

7. Y.-L.S. Tse, C. Knight, and G.A. Voth, *An analysis of hydrated proton diffusion in ab initio molecular dynamics*. The Journal of chemical physics **142**(1): 014104 (2015).
8. F. Dahms, R. Costard, E. Pines, B.P. Fingerhut, E.T. Nibbering, and T. Elsaesser, *The Hydrated Excess Proton in the Zundel Cation H₅O₂⁺: The Role of Ultrafast Solvent Fluctuations*. Angewandte Chemie International Edition **55**(36): 10600-10605 (2016).
9. R. Biswas, W. Carpenter, G.A. Voth, and A. Tokmakoff, *Molecular modeling and assignment of IR spectra of the hydrated excess proton in isotopically dilute water*. The Journal of Chemical Physics **145**(15): 154504 (2016).
10. M. Thämer, L. De Marco, K. Ramasesha, A. Mandal, and A. Tokmakoff, *Ultrafast 2D IR spectroscopy of the excess proton in liquid water*. Science **350**(6256): 78-82 (2015).
11. C.T. Wolke, J.A. Fournier, L.C. Dzugas, M.R. Fagiani, T.T. Odbadrakh, H. Knorke, K.D. Jordan, A.B. McCoy, K.R. Asmis, and M.A. Johnson, *Spectroscopic snapshots of the proton-transfer mechanism in water*. Science **354**(6316): 1131-1135 (2016).
12. C.M. Johnson and S. Baldelli, *Vibrational sum frequency spectroscopy studies of the influence of solutes and phospholipids at vapor/water interfaces relevant to biological and environmental systems*. Chemical Reviews **114**(17): 8416-46 (2014).
13. T. Ishiyama, T. Imamura, and A. Morita, *Theoretical Studies of Structures and Vibrational Sum Frequency Generation Spectra at Aqueous Interfaces*. Chemical reviews **114**(17): 8447-8470 (2014).
14. A.E. Stearn and H. Eyring, *The deduction of reaction mechanisms from the theory of absolute rates*. The Journal of Chemical Physics **5**(2): 113-124 (1937).
15. G. Wannier, *Die Beweglichkeit des Wasserstoff- und Hydroxylions in wässriger Lösung. I*. Annalen der Physik **416**(6): 545-568 (1935).
16. M.L. Huggins, *Hydrogen bridges in ice and liquid water*. The Journal of Physical Chemistry **40**(6): 723-731 (1936).
17. M. Eigen, *Proton Transfer, Acid-Base Catalysis, and Enzymatic Hydrolysis. Part I: ELEMENTARY PROCESSES*. Angewandte Chemie International Edition in English **3**(1): 1-19 (1964).
18. G. Zundel, P. Schuster, G. Zundel, and C. Sandorfy, *The Hydrogen Bond*. Recent developments in theory and experiments **2** (1976).
19. D. Marx, M.E. Tuckerman, J. Hutter, and M. Parrinello, *The nature of the hydrated excess proton in water*. Nature **397**(6720): 601-604 (1999).
20. S.T. Roberts, P.B. Petersen, K. Ramasesha, A. Tokmakoff, I.S. Ufimtsev, and T.J. Martinez, *Observation of a Zundel-like transition state during proton transfer in aqueous hydroxide solutions*. Proceedings of the National Academy of Sciences of the United States of America **106**(36): 15154-15159 (2009).
21. W.J. Xie and Y.Q. Gao, *A Simple Theory for the Hofmeister Series*. J. Phys. Chem.Lett.: 4247-4252 (2013).
22. K.D. Collins, *Why continuum electrostatics theories cannot explain biological structure, polyelectrolytes or ionic strength effects in ion-protein interactions*. Biophysical chemistry **167**: 43-59 (2012).
23. K.D. Collins, *Charge density-dependent strength of hydration and biological structure*. Biophysical Journal **72**(1): 65-76 (1997).
24. X. Liu, H. Li, R. Li, D. Xie, J. Ni, and L. Wu, *Strong non-classical induction forces in ion-surface interactions: General origin of Hofmeister effects*. Sci. Rep. **4**: 9 (2014).
25. T.T. Duignan, D.F. Parsons, and B.W. Ninham, *Collins's rule, Hofmeister effects and ionic dispersion interactions*. Chemical Physics Letters **608**: 55-59 (2014).
26. F. Hofmeister, *Zur Lehre von der Wirkung der Salze*. Archiv f. experiment. Pathol. u. Pharmakol **24**(25): 1-30 (1970).

27. W.M. Cox and J.H. Wolfenden, *The Viscosity of Strong Electrolytes Measured by a Differential Method*. Vol. 145. 1934. 475-488.
28. P. Ball and J.E. Hallsworth, *Water structure and chaotropy: their uses, abuses and biological implications*. Physical chemistry chemical physics : PCCP **17**(13): 8297-305 (2015).
29. K.D. Collins and M.W. Washabaugh, *The Hofmeister effect and the behaviour of water at interfaces*. Quarterly Reviews of Biophysics **18**(04): 323-422 (1985).
30. J.D. Smith, R.J. Saykally, and P.L. Geissler, *The Effects of Dissolved Halide Anions on Hydrogen Bonding in Liquid Water*. Journal of the American Chemical Society **129**(45): 13847-13856 (2007).
31. R. Li, Z. Jiang, F. Chen, H. Yang, and Y. Guan, *Hydrogen bonded structure of water and aqueous solutions of sodium halides: a Raman spectroscopic study*. Journal of Molecular Structure **707**(1-3): 83-88 (2004).
32. M. Druchok and M. Holovko, *Structural changes in water exposed to electric fields: A molecular dynamics study*. Journal of Molecular Liquids **212**: 969-975 (2015).
33. D. Hollas, O. Svoboda, and P. Slaviček, *Fragmentation of HCl-water clusters upon ionization: Non-adiabatic ab initio dynamics study*. Chemical Physics Letters **622**: 80-85 (2015).
34. Y. Gong, Y. Zhou, H. Wu, D. Wu, Y. Huang, and C.Q. Sun, *Raman spectroscopy of alkali halide hydration: hydrogen bond relaxation and polarization*. Journal of Raman Spectroscopy: DOI: 10.1002/jrs.4963 (2016).
35. X. Zhang, T. Yan, Y. Huang, Z. Ma, X. Liu, B. Zou, and C.Q. Sun, *Mediating relaxation and polarization of hydrogen-bonds in water by NaCl salting and heating*. Physical Chemistry Chemical Physics **16**(45): 24666-24671 (2014).
36. X. Zhang, Y. Zhou, Y. Gong, Y. Huang, and C. Sun, *Resolving H(Cl, Br, I) capabilities of transforming solution hydrogen-bond and surface-stress*. Chemical Physics Letters **678**: 233-240 (2017).
37. X. Zhang, Y. Xu, Y. Zhou, Y. Gong, Y. Huang, and C.Q. Sun, *HCl, KCl and KOH Solvation Resolved Solute-Solvent Interactions and Solution Surface Stress* Applied Surface Science **10.1016/j.apsusc.2017.06.0190169-4332/** (2017).
38. C.Q. Sun and Y. Sun, *The Attribute of Water: Single Notion, Multiple Myths*. Springer Ser. Chem. Phys. Vol. 113. 2016, Heidelberg: Springer-Verlag. 494 pp.
39. Y. Zhou, D. Wu, Y. Gong, Z. Ma, Y. Huang, X. Zhang, and C.Q. Sun, *Base-hydration-resolved hydrogen-bond networking dynamics: Quantum point compression*. Journal of Molecular Liquids **223**: 1277-1283 (2016).
40. C.Q. Sun, X. Zhang, J. Zhou, Y. Huang, Y. Zhou, and W. Zheng, *Density, Elasticity, and Stability Anomalies of Water Molecules with Fewer than Four Neighbors*. Journal of Physical Chemistry Letters **4**: 2565-2570 (2013).
41. X. Zhang, P. Sun, Y. Huang, T. Yan, Z. Ma, X. Liu, B. Zou, J. Zhou, W. Zheng, and C.Q. Sun, *Water's phase diagram: from the notion of thermodynamics to hydrogen-bond cooperativity*. Progress in Solid State Chemistry **43**: 71-81 (2015).
42. Q. Zeng, T. Yan, K. Wang, Y. Gong, Y. Zhou, Y. Huang, C.Q. Sun, and B. Zou, *Compression icing of room-temperature NaX solutions (X= F, Cl, Br, I)*. Physical Chemistry Chemical Physics **18**(20): 14046-14054 (2016).
43. F. Hofmeister, *Concerning regularities in the protein-precipitating effects of salts and the relationship of these effects to the physiological behaviour of salts*. Arch. Exp. Pathol. Pharmacol **24**: 247-260 (1888).
44. J. Peng, J. Guo, R. Ma, X. Meng, and Y. Jiang, *Atomic-scale imaging of the dissolution of NaCl islands by water at low temperature*. Journal of Physics: Condensed Matter **29**(10): 104001 (2017).

45. S.A. Harich, D.W.H. Hwang, X. Yang, J.J. Lin, X. Yang, and R.N. Dixon, *Photodissociation of H₂O at 121.6 nm: A state-to-state dynamical picture*. *The Journal of chemical physics* **113**(22): 10073-10090 (2000).
46. X. Wu, W. Lu, W. Ou, M.C. Caumon, and J. Dubessy, *Temperature and salinity effects on the Raman scattering cross section of the water OH-stretching vibration band in NaCl aqueous solutions from 0 to 300° C*. *Journal of Raman Spectroscopy* **10.1002/jrs.5039** (2016).
47. G. Jones and M. Dole, *The viscosity of aqueous solutions of strong electrolytes with special reference to barium chloride*. *Journal of the American Chemical Society* **51**(10): 2950-2964 (1929).
48. Y. Zhou, Y. Huang, Z. Ma, Y. Gong, X. Zhang, Y. Sun, and C.Q. Sun, *Water molecular structure-order in the NaX hydration shells (X= F, Cl, Br, I)*. *Journal of Molecular Liquids* **221**: 788-797 (2016).